Charge Fraction Measurements for Heavy Particle Beams Generated by the Tandem Accelerator with MCP System*)

Akira TANIIKE, Tomoaki SHINOBU, Sho MOCHIZUKI, Takeshi IDO[1)], Akihiro SHIMIZU[1)], Masaki NISHIURA[1)] and Yuichi FURUYAMA

Graduate School of Maritime Sciences, Kobe University, 5-1-1 Fukaeminami-machi, Higashinada-ku, Kobe 658-0022, Japan

[1)]*National Institute for Fusion Science, 322-6 Oroshi-cho, Toki 509-5292, Japan*

(Received 21 November 2012 / Accepted 8 May 2013)

In order to expand the applied range of the heavy ion beam probe measurement on LHD, it is important to increase the probing beam current. A method of increasing the current is the improvement of charge exchange efficiency of a gas cell. The experiments were carried out on a tandem accelerator at Kobe University, 5SDH-2, because various conditions of experiments can be selected for gas species, gas pressure, and ion energy. Charge fractions of negative ion, neutral atom and the positive ions were measured by a micro channel plate or Faraday cup. Dependence of the fractions of Au^-, Au^0, Au^+ and Au^{2+} on gas thickness was measured. Results were compared with prior calculations, and a solution of rate equations. The cross sections for ionizing and electron capture were calculated, and some cross sections were obtained from experiments. The dependence of charge fractions for Au^0, Au^+ and Au^{2+} on the gas thickness was well presented.

Keywords: Au^- ion beam, gas cell, ionization, tandem accelerator, HIBP, LHD, MCP

DOI: 10.1585/pfr.8.2401087

1. Introduction

The heavy ion beam probe (HIBP) method is one of a method of plasma diagnostics, which can measure the potential distribution in plasma. An HIBP system has been installed at the Large Helical Device (LHD-HIBP) [1]. After incident singly charged ions (Au^+) into the plasma are ionized at the point of measure, the energy and current of doubly charged ions (Au^{2+}) ejected from the plasma are measured. The plasma potential is obtained from the difference of the energies, before/after through the plasma. The trajectory of incident ion is deflected by Lorentz force from a magnetic field for the plasma confinement. Heavy ions with energy of a mega electron volt order are needed to reach the point to measure in LHD plasma. These ions are produced by an accelerator. Au ion has been employed on LHD-HIBP, and the energy is 1.5 MeV for magnetic field of 1.5 T and 6 MeV for 3 T [2]. The accelerator is a tandem type, and the terminal voltage is 3 MV. A gas cell has been installed at the high voltage terminal for the charge stripping of negative ions.

In recent HIBP diagnostics the current of the heavy ion beam is sufficient for the electron density of $10^{19}\,m^{-3}$. Since the diagnostics could not conduct with good S/N for larger density plasma, larger Au^+ current is needed in this case. Some studies investigating how to increase the current have been done [3–5]. These objectives are to increase the negative ion beam current, the charge exchange efficiency in the gas cell, the beam transport efficiency, the detection efficiency of ejected ions and so on. The experimental study to increase the Au^+ beam current is not easy using LHD-HIBP. We have studied on the subject using a tandem accelerator at Kobe University. The accelerator has a gas cell, and the terminal voltage is up to 1.7 MV.

From the viewpoint of atomic and molecular collision physics, it is important to obtain the data of the cross sections for heavy ion. There are only some data of the collision cross sections for the heavy ion whose energy is less than a few MeV as in present case. Moreover, it is difficult to calculate the cross sections exactly, because the collision of a heavy ion is multielectron system. In this study, the charge fractions of Au beam generated by tandem accelerator were measured, and some ionization cross sections for Au ion or neutral atom were obtained.

2. Experimental Apparatus

2.1 Tandem accelerator

A tandem accelerator, the Pelletron 5SDH-2; NEC Corp., at Kobe University was used for the experiments. The accelerator has a gas cell, and the terminal voltage is up to 1.7 MV. The system is shown in Fig. 1. Negative ions of almost all elements can be produced by two ion sources. The current is measured by a Faraday cup at low energy part (LE FC). After acceleration a positive ion beam current is measured by a Faraday cup at high energy part (HE

author's e-mail: taniike@maritime.kobe-u.ac.jp

*) This article is based on the presentation at the 22nd International Toki Conference (ITC22).

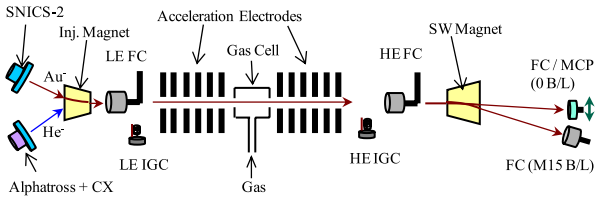

Fig. 1 Experimental apparatus with a tandem accelerator is used to measure the charge fractions for heavy ions/neutrals.

FC). Ions through a bending magnet (SW Magnet) for selection of ionic charge are detected by a FC at M15 B/L or FC/MCP at 0 B/L. These numbers indicate the deflection angle. Gas pressure is measured by an ionization gas gauge controller (IGC) at LE and HE part.

2.2 Calibration of gas thickness

Calibration of gas thickness is very important in determining the cross sections in collision reaction. As a gas gauge is not installed with a gas cell part, the gas pressure is not read directly when the accelerator is operating. The gas pressure at the part of LE IGC is not appropriate to use for calibration because many impurities come from the ion source. We try to determine the gas thickness using HE IGC. A pressure transducer, BARATRON, was temporally installed on the top of gas cell. A relation between two pressures measured by BARATRON and HE IGC for some gas species was obtained when the accelerator is not operating. On the other hand, the gas pressure distribution with the tube conductance was calculated. Since gas pressure has a linear distribution in a pipe, a gas thickness should be integrated over a gas cell taking the distribution into consideration. Finally, the gas thickness was calibrated by the two methods listed above [6].

2.3 Particle detection system with MCP

To obtain the charge fraction, measurements of the ion current are necessary. The current can be measured with a Faraday cup. Since the initial state of the ion is negative in the present work, measurement of neutral atom is also necessary. We consider the use of MCP. This is because the *initial* secondary-electrons can be produced by ions or neutral particles at the entrance section of the MCP. Two stages micro channel plate (Hamamatsu photonics Inc.) was used and set on $x-y$ movable stage. Entrance of MCP was biased at 1800 V, and exit was biased at 300 V. The collector has ground potential.

The current detected by MCP must be calibrated for absolute measurement and comparison to the FC current. Characteristics of MCP for ion species, ion charge state and ion energy was measured with the following method.

Four Faraday cups were used for this calibration. LE FC has been installed at the beam line connecting the ion source and the tandem accelerator. The LE FC current was used to normalize the other current. HE FC has been installed at the tandem accelerator and bending magnet (SW Magnet). FC1 was installed at inside of the M15 beam line chamber for this study, and can move to pass the ion beam to FC2. FC2 has been installed at the end of the M15 beam line chamber.

At first, the relationship between the currents measured with these Faraday cups was measured. The characteristics were measured for positive ions. Some experiments were conducted to obtain the currents of FC1 and the FC2. On the experiments Au^+, Au^{2+}, Cu^+, Cu^{2+} and H^+ beams were used. The energy was below 300 keV for Au, 1000 keV for Cu and 2000 keV for H^+. Because the currents of FC1 and FC2 were same in these experiments, we treated the entrance current into MCP was same as the current of FC1. In the next, the FC1 was replaced as the MCP stage, then the following experiments were conducted.

MCP gain depends on a species and the energy of incident particle. It is considered the gain is nearly proportional to the stopping power. The gain measurement was conducted in our system. The results showed the gain was around 200, and the energy dependence was obtained. Because the experiments were conducted with simple setup, the gain dependence on the incident energy was not measured in sufficient precision. The gain will have to be measured exactly in the future to obtain more accurate cross sections.

3. Experimental Results

3.1 Total ionization cross section measurement

In this section we consider the total ionization cross sections for negative gold ions. The initial energy of Au^-, E_{ni}, is 21 keV, and the energy is corresponding to acceleration voltage at the ion source. The ions pass through the tandem accelerator, whose terminal voltage is V_T, and are measured. The negative ions are accelerated in the part of low energy column in the accelerator, and the energy become $E_{ni} + eV_T$. Then the ions are decelerated by $-V_T$ at the part of high energy column, and finally the energy is E_{ni}.

In the present work, negative ion was not detected by MCP system. Since the energy of negative ions was as small as 21 keV and the part of MCP entrance was biased in negative, the negative ions were deflected by the potential, and the ions could not enter via the MCP entrance aperture. Consequently, the negative current was measured by a Faraday cup system.

Figure 2 shows attenuation curves for an Au^- ion beam. The vertical axis is the beam current normalized by LE FC. The energies in the legend represent the entrance energy to the gas cell. The Au^- ions are decreased as the gas thickness of Ar, nL, are increased. The curve is expressed as a rate equation (1),

$$\frac{dF^-}{dx} = -(\sigma_{-1,0}+\sigma_{-1,1}+\sigma_{-1,2}+\sigma_{-1,3}+\cdots+\sigma_s)F^-, \quad (1)$$

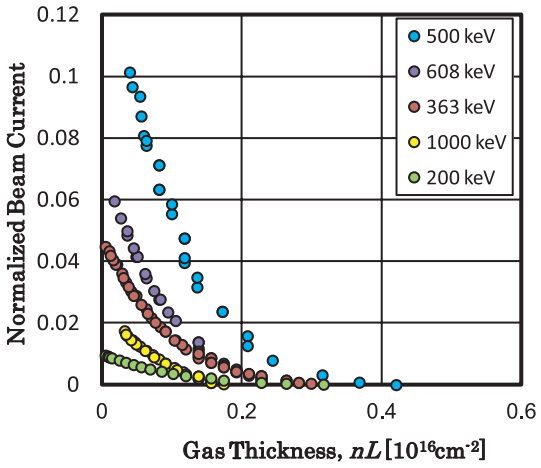

Fig. 2 Attenuation curves of Au^- ion beam current for Ar target.

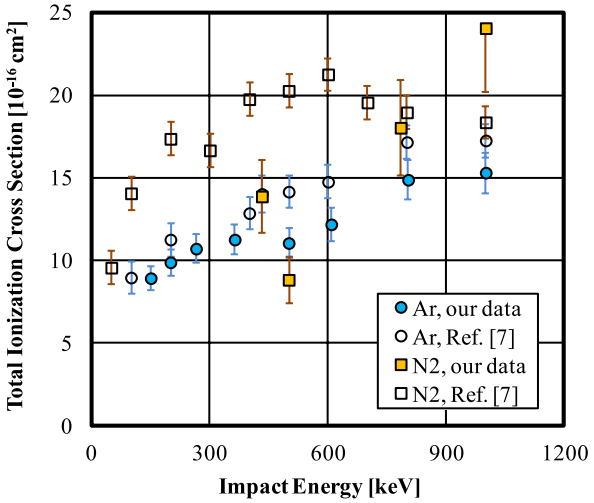

Fig. 3 Total ionization cross sections in Ref. [7] and our data.

where F^- is a fraction of a negative ion, $\sigma_{-1,0}$, $\sigma_{-1,1}$, $\sigma_{-1,2}$, and $\sigma_{-1,3}$ are the ionization cross sections. The first suffix represents the initial state of the particle and the second represents the final state in a collision. The fraction F^- is corresponding with the normalized current. σ_s is a scattering cross section and x represents the gas thickness. The exponential term of the solution is a function of $(\sigma_{-1,\text{total}} + \sigma_s)nL$. $\sigma_{-1,\text{total}}$ and σ_s represent the total ionization cross section and scattering cross section, respectively.

Figure 3 shows the ionization cross sections of Au^- ions in collisions of Ar and N_2 described in Ref. [7]. Our results obtained from the fitting curves are also shown in Fig. 3. In the case of Ar target our data are smaller than the data in Ref. [7], but show the same tendency as the energy dependence. In the case of N_2 target, the errors of our data are larger than that in Ar case, because the fitting error was a little large. The cross sections for N_2 target agree with the data of Ref. [7] by a factor of two. Since our data include the scattering cross section, the discrepancies may be larger than shown in Fig. 3. A quadruple lens system has been installed at HE beam line to focus positive ion beams. Since the negative ion beam is also focused by the lens, the acceptance angle is larger than the angle calculated with the geometry of the apparatus. The scattering cross section is explained in section 4.1.

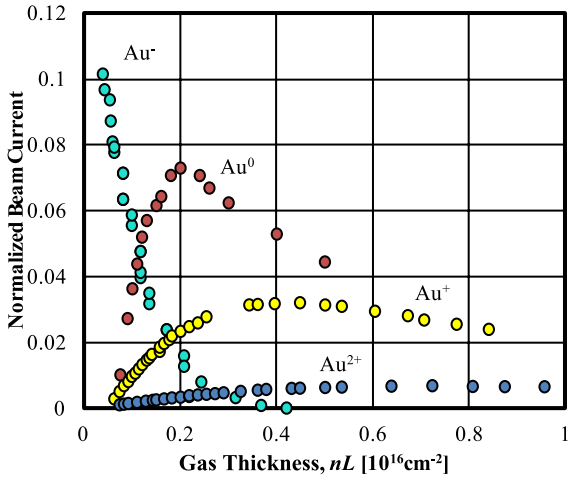

Fig. 4 Charge fractions measured with MCP and FC. Impact energy of Au^- is 500 keV, and target gas is Ar.

3.2 Charge fraction measurement

A charge fraction was measured with the MCP system at 0 B/L. Accelerated Au^- is ionized in the gas cell and becomes Au^0, Au^+, Au^{2+}, and so on through a direct or sequential process. As MCP is installed at a straight position, all species ions/atoms are entered. Neutral atom can be easily measured by deflecting away other charged particle with a SW Magnet. Ions can be also measured with SW Magnet. Since other *unfocused* charge state ions or neutrals are also detected, the detected current needs some corrections. The ion beam is focused on the MCP entrance and the current is measured. As the MCP is movable in the $x - y$ direction of ±5 mm, the beam profile is obtained. We assume the profile is a Gaussian distribution, the total current is estimated with the peak current. The profile indicates the existence of other overlapping ion profiles. The ion current is corrected as removing this overlapping current.

Figure 4 shows the dependence of Au charge fractions on Ar target thickness. The impact energy of Au^- is 500 keV. Au^0, Au^+ and Au^{2+} are measured with MCP. The output was corrected with an ion beam current with a calibration factor mentioned above. The Au^- current was measured by FC. The origin of horizontal axis is not exact, and it needs a small correction, because an influence of residual gas. The result is compared with the solution of the rate equation in section 4.4.

3.3 Estimation of ionization cross section

Some ionization cross sections are estimated from the results of Fig. 4. When a very small amount of gas is intro-

duced into the gas cell, Au^0, Au^+, Au^{2+} and other highly charged ions do not exist. Three ionization cross sections, $\sigma_{-1,0}$, $\sigma_{-1,1}$ and $\sigma_{-1,2}$ are estimated using the gradient at nL = 0. The values are 7.0×10^{-16} cm^2, 1.3×10^{-16} cm^2 and 0.15×10^{-16} cm^2 for $\sigma_{-1,0}$, $\sigma_{-1,1}$ and $\sigma_{-1,2}$, respectively. These values are compared with calculated values in section 4.2.

4. Calculations for Cross Sections

4.1 Scattering cross sections

In this section, we discuss about scattering cross sections. Ions are scattered by Coulomb force between two nuclei after a collision. This is so called an elastic collision, and an inelastic collision is simultaneously occurred [8].

The ions exit the gas cell with the scattering angle, and the maximum acceptance angle is calculated with the experimental geometry. The angle, $\Theta_{\max}$ in laboratory flame, is expressed as a following equation.

$$\Theta_{\max} = \arctan\left(\frac{r_{\text{cell}+r_{\text{ap}}}}{L}\right). \quad (2)$$

Where r_{cell} is the radius of an exit aperture in the gas cell, the r_{ap} radius is determined by the apparatus, with L as the distance between the center of the cell and a detector. We employ half of the movable distance of MCP as r_{ap}, i.e. r_{ap} = 5.00 mm. The other values of r_{cell} and L are 3.95 mm and 4226 mm, respectively. Then, $\Theta_{\max}$ is 2.12×10^{-3} degree.

Maximum acceptance angle, $\theta_{\max}$ in the center of the mass coordinate can be converted with Θ_{max}, projectile mass, M_{p}, and target mass, M_{t}, as the next equation illustrates.

$$\theta_{\max} = \theta_{\max} + \arcsin\left(\frac{M_{\text{p}}}{M_{\text{t}}} \sin\theta_{\max}\right). \quad (3)$$

The minimum impact parameter, $b_{\min}$, which corresponds to the maximum acceptance angle can be calculated as described in Ref. [8]. Finally, scattering cross sections σ_{s} are simply expressed as $\sigma_{\text{s}} = \pi b_{\min}^2$. The minimum impact parameter, $b_{\min}$, is computed as 0.775×10^{-8} cm, and the scattering cross section, σ_{s}, is 1.89×10^{-16} cm^2.

4.2 Ionization cross sections

Projectile ion receiving sufficient energy from target atoms for ionizing can be ionized. The energy transfer depends on the impact parameter written in Ref. [8]. The ionization cross section can be calculated by Firsov's equation [9]. The values have an uncertainty by a factor of two. As some ionization cross sections were obtained experimentally as mentioned above. The comparison is shown in Table 1.

4.3 Electron capture cross sections

The electron capture and recombination cross section can be calculated with the method in Ref. [9]. Since the calculated values may be slightly large, the cross sections are just used for the calculation of charge fractions in section 4.5.

Table 1 Ionization cross section for negative ion. The unit is in 10^{-16} cm^2.

	$\sigma_{-1,0}$	$\sigma_{-1,1}$	$\sigma_{-1,2}$	$\sigma_{-1,3}$
Exp.	7.0	1.3	0.15	
Calc.	23	9.9	5.4	3.3

4.4 Charge fraction calculations

Charge fractions are easily calculated by solving the rate equations. Some equations are expressed as Eqs. (4) - (6). F^- is a fraction of negative ion, and F^0 is a neutral atom, F^+ is a singly charged positive ion, and so on. The variable x represents gas thickness. Some σ denote the cross sections. σ_{s} is scattering cross section. $\sigma_{i,f}$ is a cross sections with ionization/electron capture, i denotes the initial state and f denotes the final state.

$$\frac{\partial F^-}{\partial x} = -(\sigma_{-1,0}+\sigma_{-1,1}+\sigma_{-1,2}+\sigma_{-1,3}+\cdots+\sigma_{\text{s}})F^- + \sigma_{0,-1}F^0\cdots, \quad (4)$$

$$\frac{\partial F^0}{\partial x} = -(\sigma_{0,-1}+\sigma_{0,1}+\sigma_{1,2}+\sigma_{0,3}+\cdots)F^0 + \sigma_{-1,0}F^- + \sigma_{-1,0}F^+\cdots, \quad (5)$$

$$\frac{\partial F^+}{\partial x} = -(\sigma_{1,0}+\sigma_{1,2}+\sigma_{1,3}+\sigma_{1,4}+\cdots)F^+ + \sigma_{-1,1}F^- + \sigma_{0,1}F^0 + \sigma_{2,1}F^{2+}\cdots. \quad (6)$$

4.5 Comparison of measurement and calculation

Many cross sections are needed to solve the rate equations. Some cross sections for highly ionized terms are adjusted to fit the curve of the experimental data. Electron capture cross sections are calculated in Ref. [9]. The values estimated with experimental data in section 4.2 are employed as ionizing cross section for negative ion. The scattering cross section, $\sigma_{\text{s}} = 1.89 \times 10^{-16}$ cm^2 is used. The calculation result is shown in Fig. 5, and the experimental data are also shown. The data were coordinated so accordingly with the origin.

The calculated fractions for small gas thickness are in strong agreement with experimental data. Au^0 values are smaller than the experimental data at the peak, but the peaking gas thickness is almost the same. Au^+ values are smaller than the experimental data overall, and the peaking gas thickness is also different from experimental data. Au^{2+} is similar, as well. The dicscrepancy of the calculation and the experimental data is much smaller than that of our result described in Ref. [5]. The discrepancy is caused by the overestimation of the scattering cross sections. In calculation of the scattering cross sections a lens effect in the acceleration system is not considered, and the cross sections are overestimated. Therefore, these discrepancies in large gas thickness are large.

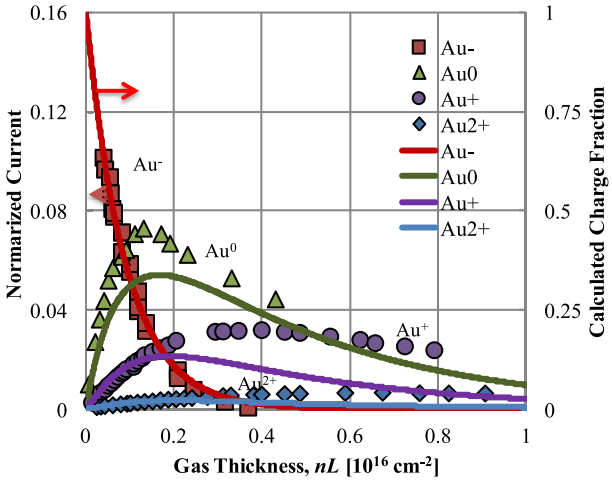

Fig. 5 Comparison of the charge fraction calculation and the experimental data.

5. Summary

In this paper, the charge fractions of Au beams for Ar target gas were discussed. The experiment was carried out with our tandem accelerator. Since a current of neutral atoms could not be measured with a Faraday cup, an MCP was used for neutral atom measurement. Ions were also measured by MCP. The dependence of charge fraction on gas thickness was measured, and was compared with the calculation of the rate equations. In the calculation some cross sections were calculated or estimated from experimental data, while others were coordinated by fitting. The dependence of charge fraction for Au^0, Au^+ and Au^{2+} on the gas thickness was well presented. Since charge fractions for various ion energy and ion species are measured using the present method, the energy dependence of the cross sections in collisions will be obtained.

Acknowledgements

This work was supported by NIFS grant NIFS12KLEH026 (2012).

[1] T. Ido *et al.*, Rev. Sci. Instrum. **77**, 10F523 (2006).
[2] T. Ido *et al.*, J. Plasma Fusion Res. **86**, 507 (2010).
[3] M. Nishiura *et al.*, Rev. Sci. Instrum. **79**, 02C713 (2008).
[4] A. Taniike *et al.*, Fusion Eng. Des. **34-45**, 675 (1997).
[5] A. Taniike *et al.*, Plasma Fusion Res. **5**, S2087 (2010).
[6] A. Taniike *et al.*, Rev. of the Faculty of Mar. Sci., Kobe Univ. **8** (2011).
[7] M.M. Sant' Anna *et al.*, Plasma Phys. Control. Fusion **51**, 045007 (2009).
[8] A. Taniike *et al.*, NIFS Report, NIFS-352 (1995).
[9] M. Nishiura *et al.*, NIFS Report, NIFS-884 (2008).